# Impact of 21st century climate change on Mississippi River Basin discharge in CESM2 large ensemble projections

Haider, M. R.; Dee, S. G.; Doss-Gollin, J.; Dunne, K. B.J.; Muñoz, S. E.

**DOI**
10.1016/j.gloplacha.2025.104742

**Publication date**
2025

**Document Version**
Final published version

**Published in**
Global and Planetary Change

Global and Planetary Change 249 (2025) 104742

Contents lists available at ScienceDirect

Global and Planetary Change

journal homepage: www.elsevier.com/locate/gloplacha

Invited Research Article

# Impact of 21st century climate change on Mississippi River Basin discharge in CESM2 large ensemble projections

M.R. Haider [a,*], S.G. Dee [b], J. Doss-Gollin [c], K.B.J. Dunne [d], S.E. Muñoz [e,f]

[a] Department of Civil Engineering, The University of Texas at Arlington, TX, USA
[b] Department of Earth, Environmental and Planetary Sciences, Rice University, Houston, TX, USA
[c] Department of Civil and Environmental Engineering, Rice University, Houston, TX, USA
[d] Department of Hydraulic Engineering, Delft University of Technology, Delft, the Netherlands
[e] Department of Marine & Environmental Sciences, Northeastern University, Marine Science Center, Nahant, MA, USA
[f] Department of Civil & Environmental Engineering, Northeastern University, Boston, MA, USA

ARTICLE INFO

Editor: Dr. Jed O Kaplan

*Keywords:*
Mississippi River
CESM2 large ensembles
Emissions scenario
Hydroclimate variability

ABSTRACT

The Mississippi River Basin (MRB), the fourth-largest river basin in the world, is an important corridor for hydroelectric power generation, agricultural and industrial production, riverine transportation, and ecosystem goods and services. Historically, flooding of the Mississippi River has resulted in significant economic losses. In a future with an intensified global hydrological cycle, the altered discharge of the river may jeopardize communities and infrastructure situated in the floodplain. This study utilizes output from the Community Earth System Model version 2 (CESM2) large ensemble simulations spanning 1930 to 2100 to quantify changes in future MRB discharge under a high greenhouse gas emissions scenario (SSP3–7.0). The simulations show that increasing precipitation trends exceed and dominate increased evapotranspiration (ET), driving an overall increase in total discharge in the Ohio and Lower Mississippi River basins. On a seasonal scale, reduced spring snowmelt is projected in the Ohio and Missouri River basins, leading to reduced spring runoff in those regions. However, decreased snowmelt and spring runoff is overshadowed by a larger increase in projected precipitation minus ET over the entire basin and leads to an increase in mean river discharge. This increase in discharge is linked to a relatively small increase in the magnitude of extreme floods (2 % and 3 % for 100-year and 1000-year floods, respectively) by the late 21st century relative to the late 20th century. Our analyses imply that under SSP3–7.0 forcing, the Mississippi River and Tributaries (MR&T) project design flood would not be exceeded at the 100-year return period. Our results harbor implications for water resources management including increased vulnerability of the Mississippi River given projected changes in climate.

## 1. Introduction

The Mississippi River Basin (MRB) drains 41 % of the contiguous United States (Rajib et al., 2021) and is home to nearly one-third of the population of the United States. The basin is one of the most productive agricultural regions in the world (Kolpin, 2000) and supports a vast network of ecosystem goods and services (Barnett et al., 2016). The Mississippi river forms an important thoroughfare for transportation that has been engineered to maintain a navigable channel, generate electricity, and protect floodplain infrastructure and communities from flooding. The lower MRB is an alluvial plain of nearly 90,650 km$^2$ straddling the river, and remains vulnerable to flooding despite the establishment of levees and spillways in the early and mid-20th century. A major flood of the lower Mississippi River valley in 1927 resulted in federal investment in flood mitigation, including the authorization of the Mississippi River and Tributaries (MR&T) project, a system of artificial spillways, levees, and dykes designed to improve navigation and reduce flood risk (DeHaan et al., 2012; Alexander et al., 2012). The MR&T project was designed to tolerate a design flood based on early and mid-20th century events and it is unclear how applicable that design flood will be to the future given climate change.

Flooding in a large basin can emerge from the interactions of several drivers including climate change, human intervention on the river system, and land cover changes (Tao et al., 2014; Slater et al., 2015; Munoz and Dee, 2017; Munoz et al., 2018; Dunne et al., 2022). Prior work has explored the impacts of climate change (Jha, 2004; Qian et al., 2007;

* Corresponding author.
*E-mail address:* rezaulwre@gmail.com (M.R. Haider).

https://doi.org/10.1016/j.gloplacha.2025.104742
Received 13 June 2023; Received in revised form 19 January 2025; Accepted 7 February 2025
Available online 15 February 2025

Rossi et al., 2009), land-use land-cover change (Schilling et al., 2008; Schilling et al., 2010), and river engineering (Pinter and Heine, 2005; Pinter et al., 2008; Pinter et al., 2010) on flooding in the MRB, including their combined effects (Foley et al., 2004; Pinter et al., 2008; Mishra et al., 2010; Frans et al., 2013). However, these works have yielded divergent conclusions regarding the primary drivers of increased flooding in the basin. For example, Pinter et al., 2008 provided evidence showing structural interventions as the largest contributor to increased flooding followed by climate and/or land-cover change. Frans et al., 2013 found climate change to be the main driver of runoff change in the upper MRB based on both modeling and hydroclimatic data analyses. In a basin-average analysis of the MRB from 1948 to 2004, Qian et al., 2007 reported an increasing trend in observed precipitation which is partly compensated by an increase in simulated ET resulting in a net increase of observed runoff.

Broadly, climate change has been shown to alter the river's flow regimes as well as the magnitude and frequency of extreme flooding events in the MRB (e.g., Lewis et al., 2022). Extreme precipitation events are projected to become more frequent over the MRB in the 21st century (Trenberth, 1999; Prudhomme et al., 2014; Lewis, 2019). At the same time, warming is expected to decrease snowmelt and increase ET (Peterson et al., 2013; Georgakakos et al., 2014). Thus, there remains significant uncertainty surrounding how the Mississippi River and its tributaries will respond to greenhouse forcing. Diverse 21st century outcomes are simulated by different climate models in terms of future discharge in the MRB, ranging from decreases (Huang et al., 2018; van der Wiel et al. 2018) to increases (Pinter et al., 2008; Tao et al., 2014; Lewis et al., 2022). A fully coupled global climate model (GCM) based study by van der Wiel et al. (2018) revealed no trend of the 100-year floods and highlighted the need for more detailed experiments with the GCM. Based on climate model simulations from CESM1.2, Dunne et al., 2022 showed an overwhelming increase in future flooding under the RCP8.5 forcing scenario in the 21st century. Disparities in model set-up, forcing scenario, and spatial and temporal resolution all contribute to diverse outcomes in projections, which makes it complicated to evaluate the influence of climate change on river discharge (Dunne et al., 2022).

How can we reduce uncertainty in these disparate projections of future MRB hydroclimate and river flows? Uncertainty in such climate change projections stems from three main sources: forcing scenario (e.g., future carbon emissions levels), model formulation (e.g., structural uncertainty, or differences in various physics or model parameterizations), and internal climate variability (Hawkins and Sutton, 2009). The "model formulation" or structural component of climate uncertainty is potentially reducible as the model improves over time, and can be assessed via the comparison of multiple climate models. Thus, multi-model ensemble experiments have also been used in previous work to explore future hydroclimate changes in future simulations. The Coupled Model Intercomparison Project Phase 6 (CMIP6) models are available with typical ensemble sizes of 3 to 10 members. However, a vast majority of the models provide only a single member. For example, recent work considers one realization per climate model either with a single scenario (e.g., Villarini and Zhang, 2020; Martel et al., 2022; Zheng et al., 2022) or multiple scenarios (e.g., Aguayo et al., 2021; Bian et al., 2023) to assess climate change effect on hydrology. In a recent study by Vieira et al. (2023), 18 GCMS were used to assess the hydrological drought on a global scale. These and other studies are limited by the fact that a single GCM run or a small ensemble size in a model precludes making a robust climate risk management decision (Deser et al., 2020). Again, multi-model ensembles using many GCMs often include both structural and forcing uncertainty, deconvolving the impact of internal variability alone is not always possible (Mankin et al., 2020).

Internal variability in the climate system has a large influence on long-term hydroclimate, and thus the full range of internal climate variability must be constrained to inform adaptation and decision-making in the coming decades (Mankin et al., 2015). An established method for capturing the range of natural variability in GCM simulations is via the use of multiple ensemble members run over the same time period with the same external forcing in the same GCM (Deser et al., 2012; Mudryk et al., 2014). Small perturbations applied to the atmosphere propagate to form large differences amongst ensemble members in their representations of internal variability (Deser et al., 2012; Kay et al., 2015; Deser et al., 2020). Large ensembles (LENS) (Kay et al., 2015) provide avenues for quantifying uncertainty due to the spread of internal climate variability. Such ensemble experiments have been widely applied to explore hydroclimate variability in global or local contexts (Hanittinan et al., 2020; Ma et al., 2020; Kumar et al., 2023). While projections of different hydroclimate variables such as precipitation and ET are regularly evaluated in GCMs, integrated river routing modules are lacking in IPCC-class models. To date, only a few studies have utilized ensembles from the Community Earth System Model (CESM, Otto-Bliesner et al., 2016), which (critically) is coupled with a river transport module (RTM, Branstetter, 2003) for analyzing changes in river discharge (Munoz and Dee, 2017; Wiman et al., 2021).

In this study we build upon previous work using CESM's river routing capabilities and a new large ensemble to address some of these gaps. We analyze the model outputs from the recently published Community Earth System Model v2 (CESM2) Large Ensemble (LENS2) (Danabasoglu et al., 2020; Rodgers et al., 2021). CESM2 LENS2 projections are available with 40 (50) ensemble members for daily (monthly) temporal resolution for SSP3–7.0 emission scenario. Specifically, we use this 50-member ensemble of river discharge data based on the simulations performed for 1850–2100. Critically, CESM2 has a fully-integrated river routing model, which allows us to evaluate changes in simulated river discharge across the MRB directly. The CESM1's RTM has been replaced with a physically based river routing model, the Model for Scale Adaptive River Transport (MOSART, Li et al., 2013; Li et al., 2015), and integrated into CESM2 (Danabasoglu et al., 2020). Simulated discharge from CESM2 coupled with MOSART has recently been utilized for the analysis of low flows in the Mississippi River (Muñoz et al., 2023). However, to date, no study has evaluated the performance of CESM2's surface hydroclimate with MOSART simulations to analyze projected change in river discharge 1) in the context of high-flows and flooding across the Mississippi basin in the past and future, and 2) to explore in detail the monthly-to-seasonal hydroclimate drivers of flooding in the basin and its regional heterogeneity across the tributary basins. Here, we report on future changes in the magnitude and frequency of extreme flooding in the MRB resulting from climate change. Our goal is to provide constraints on both changes in the magnitude of discharge, and the overall sign of hydroclimate change across each tributary basin. We explicitly address the following questions: 1) How well does the CESM2 LENS simulate observed Mississippi River discharge (means, extremes, and seasonality) in the historical period? 2) How do Mississippi River discharge statistics change under SSP3–7.0 during the 21st century? 3) How do the various components of the hydrological cycle contribute to changes in discharge in each tributary basin under the high emissions scenario? 4) How does the seasonality of hydroclimate drivers affect discharge changes over the tributary basins? and 5) Does the future flooding exceed the design discharge of the MR&T project? By evaluating changes in basin hydroclimate coupled to a river routing model within a large climate model ensemble, we aim to provide a new perspective on future hydroclimate changes in a warming climate.

## 2. Methods

This section first provides a description of the LENS2 simulations, the river routing model (MOSART), and how the dataset for each hydroclimate variable is post-processed for the tributary basins within the MRB. Then the available instrumental stream gauge dataset and calculation of different statistics are mentioned.

### 2.1. Simulated river flow and hydroclimate data

To investigate the hydrological drivers of discharge changes in the MRB, we use simulations from the Community Earth System Model, Version 2 (CESM2), the second generation of the Earth System Model developed at the National Center for Atmospheric Research (Danabasoglu et al., 2020). CESM2 is an open source and fully coupled general circulation model (GCM) which consists of a large ensemble (100-members) dataset designated as LENS2 (Rodgers et al., 2021). The spatial resolution of LENS2 is ~1°. Based on the CMIP6 biomass burning emissions protocol, we extract 50 member ensembles for 1850–2014 subject to historical emissions and for 2015–2100 subject to the future SSP3–7.0 emissions. We also use the simulated river discharge data from the Model for Scale Adaptive River Transport (MOSART, Li et al., 2015; H. Li et al., 2013), a river routing model integrated into CESM2. Critically, MOSART in CESM2 calculates river flow rates by applying the kinematic wave method, which is based on the conservation of mass and momentum (Danabasoglu et al., 2020). MOSART is an improvement over the river transport module (RTM; Branstetter, 2003) of CESM1, which uses a simple linear reservoir method where the water fluxes are calculated based on the storage volume in the upstream grid cell, the mean distance between the grid cells, and a globally constant effective flow velocity (Danabasoglu et al., 2020). Thus, MOSART simulates the river flow velocity and water depth as a function of time, which captures the streamflow seasonality and annual maximum flood (Li et al., 2015; Li et al., 2013).

While CESM2's simulation of discharge absolute values is biased and cannot be used directly for engineering decisions, its physics and simulation of overland hydrology and climate forcing relationships is robust (O'Donnell et al., 2024). Our goal is not to use the model to predict, for example, the true volume of flows on the lower Mississippi. Rather, our objective is to evaluate relative changes in discharge projected over the 21st century and the drivers of these changes. The atmospheric fields of CESM2 have been validated in previous work (e.g., Konstali et al., 2024; O'Donnell et al., 2024; Coelho et al., 2022), and thus we assert that our results exploring the hydroclimatic drivers of future flows in the river basin are reliable. Furthermore, CESM2, with its updated hydrologic routing model MOSART, has recently been reported to more skillfully simulate the observed seasonality of runoff in the MRB compared to other CMIP6 models considered (O'Donnell et al., 2024).

The monthly LENS2 dataset during the historical (1930–2014) and future (2015–2100) periods are available with a sample size of 1020 (85 × 12) and 1032 (86 × 12) months, respectively. We extract monthly discharge as well as precipitation, evapotranspiration (ET), snowmelt, soil moisture, and runoff (see Table S1 for the variable IDs) from the LENS2 dataset.

### 2.2. Study area and post-processing of hydroclimate variables

The MRB extends from the source of the Mississippi River at Lake Itasca in Minnesota to the Mississippi River Delta in the Gulf of Mexico, covering south-central North America (Fig. 1). With a catchment area of 3.24 million km$^2$ (Yin et al., 2023), the MRB is the 4th largest river in the world. The river is ultimately joined by hundreds of tributaries, including five main tributary basins, the Upper MRB, the Missouri River Basin, the Arkansas River Basin, the Ohio River Basin, and the Lower MRB representing approximately 17, 45, 15, 15, and 8 %, respectively, of the total catchment area (Rossi et al., 2009; Meade and Moody, 2009; and Yin et al., 2023).

Average annual precipitation varies from 400 mm in the northwest to 1100 mm in the southeast part of the basin (Pitlick, 1997). Based on NOAA Climate Prediction Center (CPC) data (NOAA PSL, 2016), basin average annual precipitation over the MRB has shifted during the 20th century from 737 (±80) mm during 1948–1977 to 789 (±64) mm during 1978–2007 (Fig. S1). The 20th, 50th, and 80th percentiles of the basin-average annual precipitation show an increase of 11, 7, and 5 %,

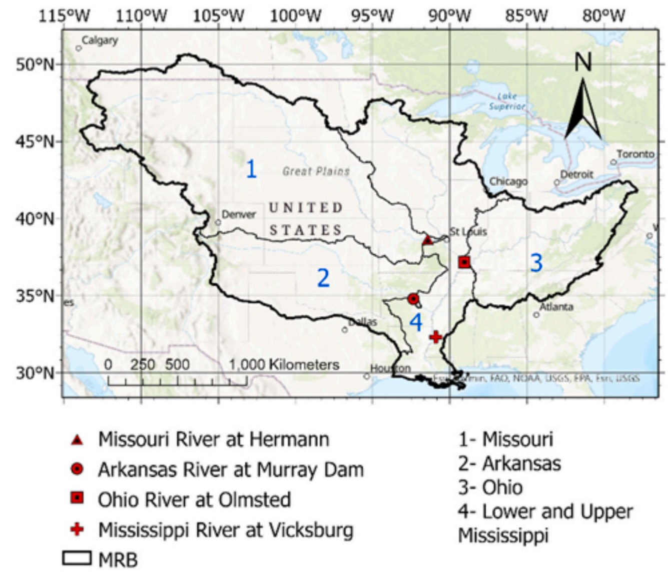


**Fig. 1.** Study area showing the MRB together with the tributary basins. Selected instrumental gauge station is shown in red marker. The distribution of precipitation averaged over the MRB is shown in Fig. S1. (For interpretation of the references to colour in this figure legend, the reader is referred to the web version of this article.)

respectively, during 1978–2007 compared to those during 1948–1977 (Fig. S1).

The simulated raster data (Rodgers et al., 2021) at each time step for the hydroclimate variables is first accessed from the Globally Accessible Data Environment (GLADE, https://arc.ucar.edu/knowledge_base/68878466) repository of the National Center for Atmospheric Research. The raster time series for each hydroclimate variable other than discharge is then masked to the shape file (USGS, 2022) for each tributary basin and a basin-average value was calculated for each variable.

### 2.3. Instrumental stream gauge data

To investigate the observed trends of river discharge in the MRB, we employ daily data available from USGS (USGS, 2023) stream gauges (Fig. 1 map, red markers). We calculate monthly average discharge for each site using the daily time series. The sites (Table S2) are selected such that each gauge is located towards the outlet of each tributary basin. The simulated discharge within the model grid cell corresponding to the gauge location is extracted and compared with observed discharge.

### 2.4. Validation of MOSART and CESM2 river discharge

An earth system model like CESM2 serves as a tool to explore the relationships between hydroclimate and streamflow. These model simulations are not intended to reproduce observed streamflow values, but robust simulations should reflect observed seasonality of streamflow and their drivers. As such, reporting the biases in the model is a necessary step in any study attempting to use a model ensemble to explore various climatic features and their impacts on river basin hydrology. Thus, here, we compare the MOSART-simulated discharge with the observed discharge for the Lower Mississippi River at Vicksburg. We build a time series of monthly average observed discharge from the daily series available from 2008 to 2024. We utilize seven years (2008–2014) from this series to include only the years intersecting with the CESM historical simulation. Then we compare the simulated and observed discharge time series on a monthly scale from 2008 to 2014. We calculated and compared mean discharge over different seasons (winter:

DJF, spring: MAM, summer: JJA, fall: SON) during 2008–2014 for the simulated and observed discharge. The bias in simulated discharge is calculated as follows:

$$Bias = \left(\frac{Q_{sim} - Q_{obs}}{Q_{obs}}\right) \times 100 \quad (i)$$

Where $Q_{sim}$ = simulated discharge, $Q_{obs}$ = observed discharge.

### 2.5. Methods: projected changes in hydroclimate

To assess future changes in hydroclimate we compare the statistics for different hydroclimate variables in the 21st century to those in the 20th Century. Three time periods spanning 30 years each (2015–2044, 2045–2074, and 2075–2100, the last period being 26 years) are chosen and designated as the early, mid and late 21st century, respectively. The statistics for each hydroclimate variable in each time period is compared with a set of historical reference years (1971–2000). The anomalies for each variable are calculated with respect to the average value during the reference period.

### 2.6. Methods: extreme value analysis

We evaluate the likelihood of extreme discharge and flooding in the Lower Mississippi River in the CESM2 large ensemble using extreme value analysis and proceed through the following steps to pre-process the data.

#### 2.6.1. Bias correction of simulated discharge data

An essential first step is to remove the systematic biases (Ivanov et al., 2018) in the GCM-simulated discharge. The bias correction method first determines the biases present in the GCM outputs by comparing them against the observations. The peak discharge per water year (October 1 through September 30) was calculated from the daily discharge for each ensemble member. This was done for the grid cell (32.315°N, 90.906°W) where the USGS gauge at Vicksburg is located. The instrumental water-year peak discharge (sample size = 93) for this station was accessed from the USGS website. Following Dunne et al., 2022, the z-score of the historical dataset was calculated and used to scale the historical data by the mean and standard deviation of the instrumental data:

$$z_{hist} = \frac{X_{hist} - \mu_{hist}}{\sigma_{hsit}} \quad (ii)$$

$$C_{hist} = z_{hist}.\sigma_I + \mu_I \quad (iii)$$

Where $z_{hist}$, $\mu_{hist}$, and $\sigma_{hist}$ are the z-score, arithmetic mean, and standard deviation of the historical discharge data, respectively; $\mu_I$ and $\sigma_I$ are the arithmetic mean and standard deviation of the water-year peak discharge time series available from the instrument data at Vicksburg, respectively; and $X_{hist}$ and $C_{hist}$ are the raw and bias-corrected historical data, respectively. Both the $X_{hist}$ and $C_{hist}$ data are of the shape 85 × 40 (number of years x ensemble size). The quantiles of the simulated and observed discharge datasets roughly align with the theoretical quantiles of a normal distribution (Fig. S2). Thus, we note that both the simulated and observed discharges at this location are approximately normally distributed.

The scenario data, $X_{scen}$, were bias-corrected using the z-score of the scenario data relative to the mean and standard deviation of the historical data, $z_{scen}$:

$$z_{scen} = \frac{X_{scen} - \mu_{hist}}{\sigma_{hsit}} \quad (iv)$$

$$C_{scen} = z_{scen}.\sigma_I + \mu_I \quad (v)$$

Where $C_{scen}$ is the bias-corrected scenario data, which is of the shape 86 × 40 (number of years x ensemble size). The bias correction of the scenario data preserves the mean and variance of the instrumental data while allowing a systematic deviation from the historical data.

#### 2.6.2. Frequency analysis of discharge data

Flood frequency analysis (FFA) of discharge was computed using Generalized Extreme Value (GEV), a distribution that consists of three parameters: location, scale, and shape. The probability density function (PDF) of the distribution is given by:

$$f(x) = \frac{1}{\alpha}\left\{1 - \xi\frac{(x-\mu)}{\alpha}\right\}^{(1-\xi)/\xi} exp\left[-\left\{1 - \xi\left(\frac{x-\mu}{\alpha}\right)\right\}^{1/\xi}\right], \xi \neq 0 \quad (vi)$$

Where μ, σ, and ξ are the location, scale, and shape parameters, respectively.

The GEV parameters (equation vi) were estimated by using the "fevd" routine in the "extRemes" (Gilleland and Katz, 2016) library of the statistical package R. The maximum-likelihood estimation method was used in fitting the discharge datasets. The best estimate of the discharge as a function of the return period was obtained using the instrumental peak discharge. The water-year peak of daily discharge was calculated using the discharge data simulated for the historical period (1930–2014) and projected for the scenario era (2015–2100). This was done for each ensemble member. Both the historical (of size 85 × 40) and scenario (of size 86 × 40) time series were converted to 1D arrays resulting in two arrays of size (3400 × 1) and (3440 × 1), respectively. The best estimate of the simulated (historical and scenario) discharge as a function of the return period was obtained using these two 1D arrays.

## 3. Results

This section first validates CESM2's simulated river flows compared to observations (3.1). We then provide an assessment of the projected changes in 21st century discharge in the MRB (3.2–3.3) and then diagnose the drivers for those changes (3.4–3.5) followed by an extreme value analysis of river discharge (3.6).

### 3.1. Validation of CESM2 river discharge

First, we compared the simulated discharge with the observation for the Lower Mississippi River at Vicksburg on a monthly scale over seven years (2008–2014), shown in Fig. 2. We used all ensemble members of simulated discharge resulting in a sample size of 84 × 50 (e.g., number of months during seven years x ensembles). The simulated river flows are in broad agreement with observations during the validation period, but do show positive biases of 38 % and 5 % at the 20th and 80th percentiles, respectively, compared to the observed discharge (Fig. 2a). Notably, positive biases indicate wetter conditions in the simulated river flow relative to observation and vice versa. The mean of the simulated discharge is 11 % higher than the mean of the observed discharge (Fig. 2a). Biases of mean simulated discharge are fairly low (4 %, 5 %, and 7 %, respectively, in winter, spring, and summer) to substantially large (44 % in fall). We also assessed the annual cycle of monthly discharge available from the USGS gauge site and compared it with that of the simulated discharge for the Mississippi River at Vicksburg (Fig. S3). We calculated the anomaly for the monthly climatology of the observed and simulated (1971–2000, 2015–2044, 2045–2074, and 2075–2100) discharge relative to the observed monthly discharge climatology. Overall, the simulated discharge captures the seasonality of observed discharge climatology at Vicksburg, but with large positive biases from August to December (Fig. S3).

### 3.2. Projected changes in monthly discharge statistics

We first compare the ensemble mean of the simulated monthly discharge distribution during the early, mid, and late 21st century

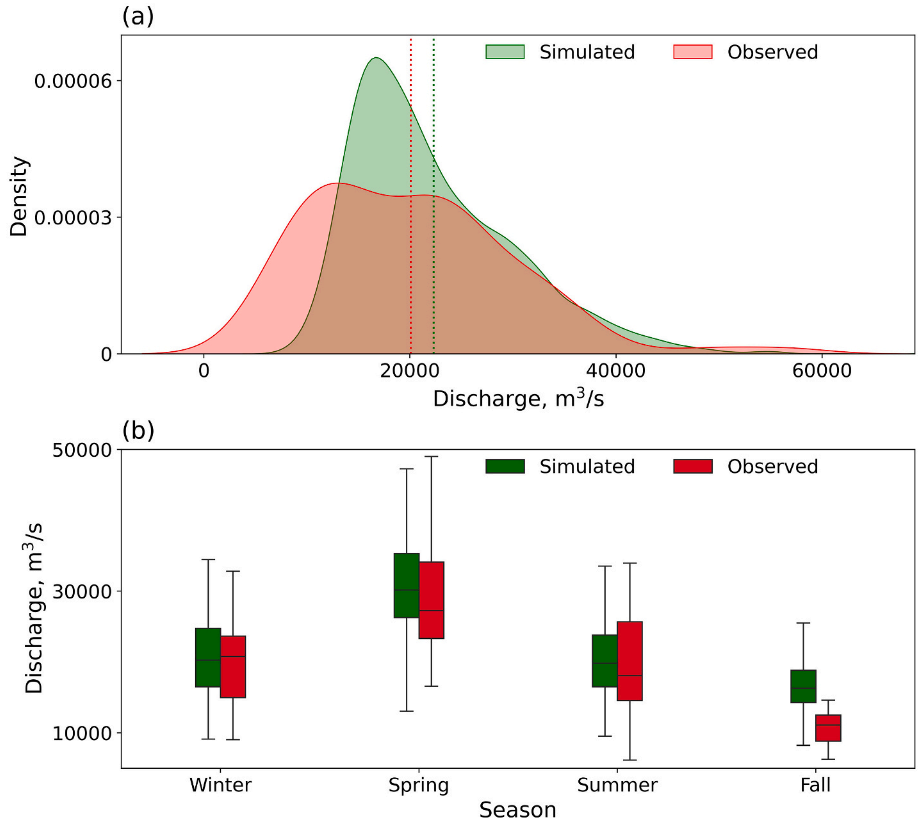


**Fig. 2.** Validation of discharge for the Lower Mississippi River at Vicksburg during the historical years with available discharge observations from USGS (2008–2014). (a) Density plot for the monthly discharge from the 50 ensemble members of CESM2 simulation and observation. The mean discharge is shown by the dotted vertical lines, (b) The box plot shows the simulated (green) and observed (red) discharge variability over different seasons during the same period. (For interpretation of the references to colour in this figure legend, the reader is referred to the web version of this article.)

relative to the mean (called reference mean) of the monthly discharge during the reference period (1971–2000) for the selected gauge sites. The mean discharges for Missouri and Arkansas are 1–10 % less (Table 1) than the reference mean values during the early, mid, and late 21st century. This is shown by the shift of the density plots towards lower discharge for these two basins (Fig. 3a, b). For Ohio and Lower Mississippi, the mean discharge in the early 21st century is up to 3 % less than the reference mean, but that in the mid-21st century is up to 4 % higher (Table 1) than the reference mean value. A relatively larger increase (5–10 %, Table 1) of the mean discharge during the late-21st century relative to the reference mean value is projected for the Ohio and Lower Mississippi River basins, noting the shift of the density plots towards higher values (Fig. 3c, d). The maximum percent change of mean discharge in the early, mid, and late 21st century is −7, −10, 5, and 10 for Missouri, Arkansas, Ohio, and the Lower Mississippi Rivers, respectively (Table 1).

The annual cycle of monthly discharge shows a wide range of variability in different months during the 21st-century relative to the reference period at selected gauge sites in the MRB (Fig. 4). Projected 21st century discharge for the Missouri River at Hermann and Ohio River at Olmsted shows a decrease up to 23 % during March to May relative to the mean discharge in the reference period (Fig. 4a, c). For the rest of the year, the early and mid 21st century discharge mostly decreases by up to 11 % and the late 21st century discharge mostly increases by as much as 12 % relative to the mean discharge during the reference period in the Missouri River. The Ohio River, for the months other than March to May, shows a minor change (within ±5 %) during the early 21st century but a larger increase (up to 20 %) during the mid and late 21st century relative to the mean discharge during the reference period (Fig. 4c). Discharge in the Arkansas River near Little Rock shows a large increase (up to 21 %) in August and a decrease (up to 14 %) for all other months (Fig. 4b).

Moreover, discharge in the Lower Mississippi River at Vicksburg shows a minor change (−6 % to 3 %) in different months of the early 21st century but large increase in the mid (up to 11 %) and late (up to 21 %) 21st century (Fig. 4d). There is a maximum reduction of discharge by 17, 23, and 21 % and a maximum increase by 5, 11, and 21 % during the early, mid and late 21st century, respectively, in the tributary basins relative to the reference period (Fig. 4). In general, discharge is projected to increase towards the late 21st century at all gauge locations analyzed here, as shown by the upward shift of the line plots moving from early to the late 21st century (Fig. 4), though we note that during March to May discharge decreases towards the late 21st century for the Missouri and Ohio Rivers.

**Table 1**
Percent difference of ensemble mean discharge during the 21st century relative to the reference period (1971–2000). Positive values indicate that the model produces higher mean discharge than that during the reference period.

| Gauge site | Early 21st century (2015–2044) | Mid 21st century (2045–2074) | Late 21st century (2075–2100) |
|---|---|---|---|
| Missouri at Hermann | −7 | −7 | −2 |
| Arkansas near Little Rock | −10 | −5 | −1 |
| Ohio at Olmsted | −3 | 0 | 5 |
| Mississippi at Vicksburg | −2 | 4 | 10 |

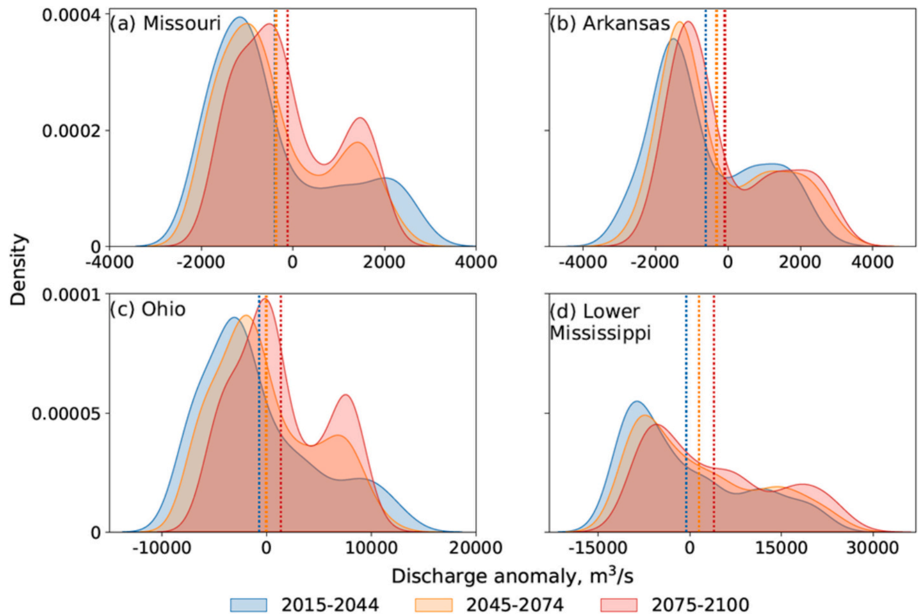


**Fig. 3.** Density plot for the ensemble mean monthly discharge anomaly from CESM2 for the early (2015–2044), mid (2045–2074) and late (2075–2100) 21st century for selected gauges: (a) Missouri at Hermann, (b) Arkansas near Little Rock, (c) Ohio at Olmsted, and (d) Lower Mississippi at Vicksburg. The mean value of the discharge anomalies during different time periods are shown by the dotted vertical lines in each panel.

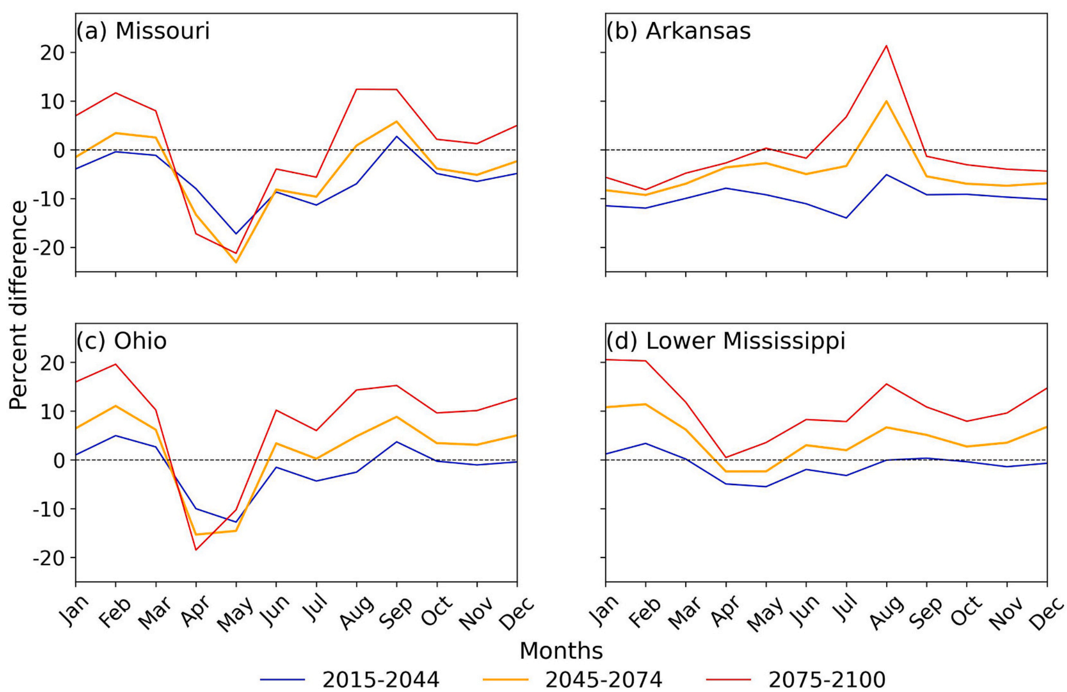


**Fig. 4.** Projected change in climatological annual cycle of discharge from CESM2 for the early, mid, and late 21st century for selected gauge stations: (a) Missouri River at Herman, (b) Arkansas River near Little Rock, (c) Ohio River at Olmsted, and (d) Lower Mississippi River at Vicksburg. Percentage change of discharge at each month is calculated relative to the ensemble mean value for that month over the historical reference period (1971–2000).

### *3.3. Projected changes in annual discharge statistics*

We compute the percent change of annual discharge time series during the historical and scenario years relative to the reference period (1971–2000) for the representative site at each tributary basin to indicate the relative influence of these basins on the Mississippi River discharge. The projection shows a decreasing trend of discharge for the Missouri and Arkansas River basins but no trend for Ohio and Lower Mississippi River basins during the early 21st century (Fig. 5a, b). The Missouri and Arkansas River basins show an increasing trend of discharge during the mid and late 21st century although the discharge magnitudes are mostly less compared to the reference period average (Fig. 5a, b). Both the Ohio and Lower Mississippi River basins show increases during the mid and late 21st century. The largest increases of mean annual discharge in the Ohio and Lower Mississippi River basins are 12 % and 17 %, respectively (Fig. 5a, b).

We also examine the influence of each tributary basin's discharge on overall lower Mississippi projected flows. Fig. S4 shows the discharge

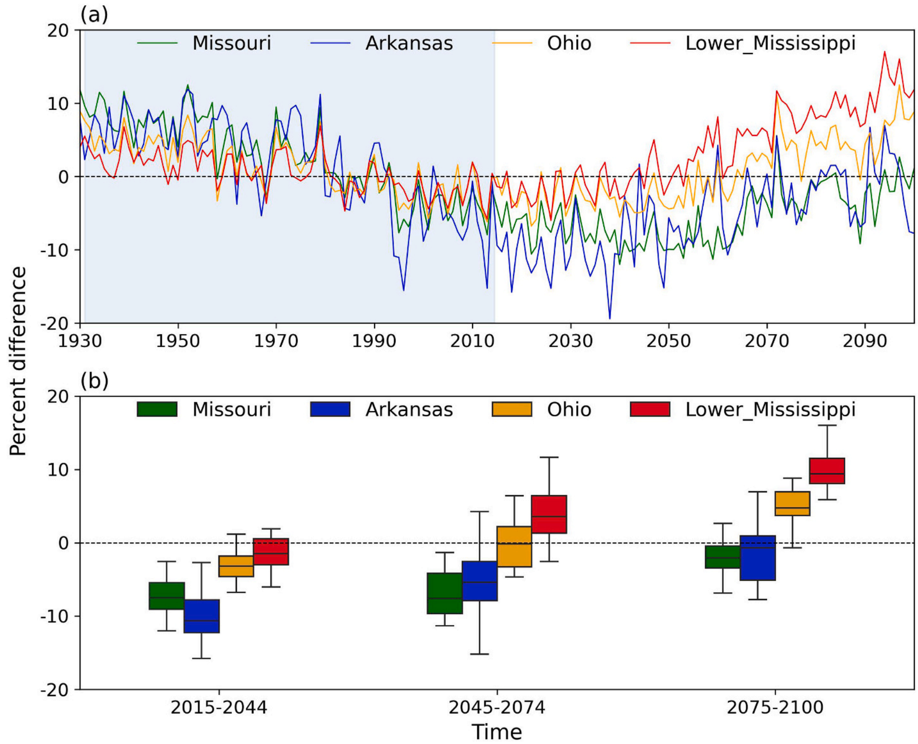


**Fig. 5.** (a) Percent change in ensemble mean of annual mean discharge relative to the reference period (1971–2000) average, (b) Projected changes for the early, mid, and late 21st century relative to the reference period.

time series for the Mississippi River at Vicksburg and at the outlet of each tributary basin for the historical and scenario years. The yearly discharge time series at each basin is normalized by dividing the discharge at each time step by the maximum value ($Q_{max}$) of the discharge time series at the Lower Mississippi River at Vicksburg. The discharge magnitudes vary between 7 and 8 %, 15–18 %, 28–34 %, and 80–100 % of the $Q_{max}$, at the Arkansas, Missouri, Ohio, and the Lower Mississippi River basin outlets, respectively (Fig. S4).

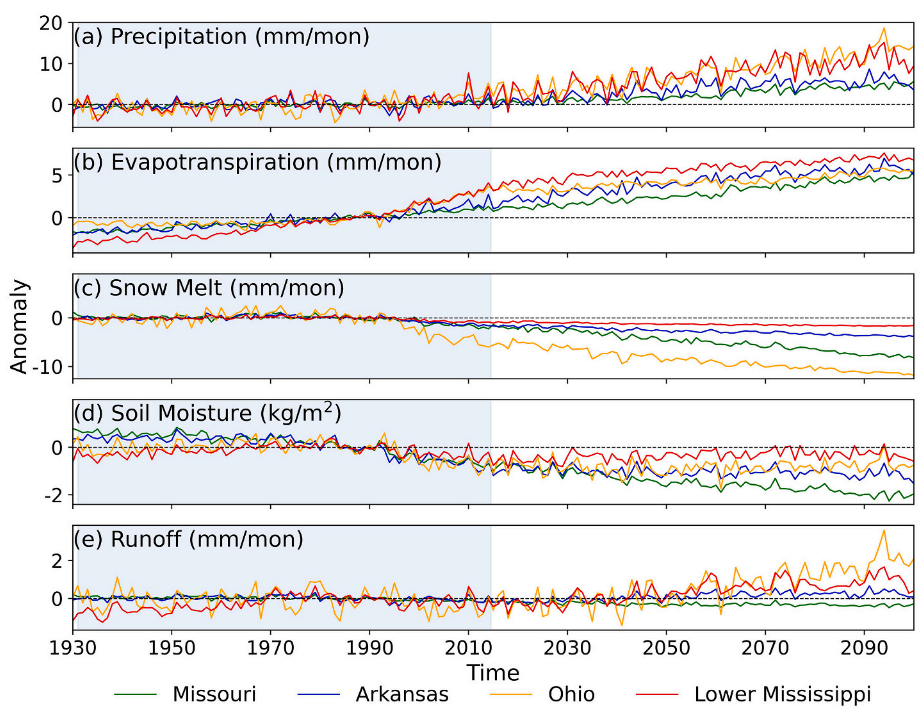


**Fig. 6.** Time series of annual mean anomalies under the historical (shaded blue) and SSP3–7.0 simulations from CESM2 for the basin average (a) precipitation, (b) evapotranspiration, (c) snow melt, (d) soil moisture, and (e) runoff. The anomalies are calculated with respect to the reference period (1971–2000). (For interpretation of the references to colour in this figure legend, the reader is referred to the web version of this article.)

### 3.4. Diagnosing the drivers of increased river discharge

#### 3.4.1. Temporal hydroclimate changes

To evaluate how the large-scale hydroclimate in CESM2 influences MRB discharge, we next analyzed temporal and spatial changes in hydrological cycle variables across the basin and throughout the 21st century (Fig. 6). Although there is no observable trend during the historical period, the basin-averaged precipitation shows an increasing trend throughout the 21st century for all the basins (Fig. 6a). The increase of precipitation during the 21st century is much higher in the Ohio and Lower Mississippi River basins compared to the Missouri and the Arkansas River basins (Fig. 6a). Importantly, the Ohio River basin shows an overwhelming increase in precipitation in the late 21st century (Figs. 6a and 7a).

The ET magnitudes show an increasing trend during the historical and scenario years for all the basins (Fig. 6b). The ET anomalies are negative from the beginning of the historical period throughout the 1970s but turn into positive values afterward that continue throughout the 21st century for all the basins. Although the Lower Mississippi River basin shows the maximum negative values of ET anomalies during the beginning of the historical years, there is a maximum increase in ET for this basin throughout the 21st century (Fig. 6b). Although no trend is observed during the historical years, snowmelt shows a decreasing trend from the late 20th century through the late 21st century for all the basins (Fig. 6c). The Ohio River basin shows the highest decrease (up to −12 mm/month) in snowmelt rate followed by a moderate decreasing rate (up to −7 mm/month) in the Missouri River basin, a nominal decreasing rate (up to −3 mm/month) in the Arkansas River basin, whereas the decreasing rate is negligible in the Lower Mississippi River basin (Fig. 6c and 7c).

The soil moisture magnitude shows a decreasing trend from the beginning of the historical years that continues throughout the 21st century for the Missouri, Arkansas, and Ohio River basins but does not show any trend for the Lower Mississippi River basin for the same time (Fig. 6d). The runoff anomalies are projected to be close to zero for the 21st century over the Missouri and the Arkansas River basins (Fig. 6e). The Ohio and the Lower Mississippi River basins are projected to have an increasing trend during the mid- and late-21st century, with the greatest increase for the Ohio River basin in the late-21st century (Figs. 6e and 7e).

#### 3.4.2. Spatial hydroclimate changes

To investigate how the spatial changes in projected hydroclimate contribute to discharge, we calculate the magnitude of change for each hydroclimatic variable in the early, mid, and late 21st centuries (Fig. 8). The change at each grid cell is calculated as the percentage change of the mean value for each variable at each time period of the 21st century (e.g., early, mid or late) with respect to the mean value of the respective variable in the reference period. The projected mean precipitation shows a moderate increase of 6 and 9 mm/month respectively over the Missouri and Arkansas River basins and a large increase of 19 and 15 mm/month respectively over Ohio and the Lower Mississippi River basins in the mid to late 21st century relative to the mean precipitation in the reference period (Fig. 8a-c). In contrast, the projected mean value of ET shows a moderate increase by 5–8 mm/month across the basins in the mid to late 21st century relative to the mean value of ET in the reference

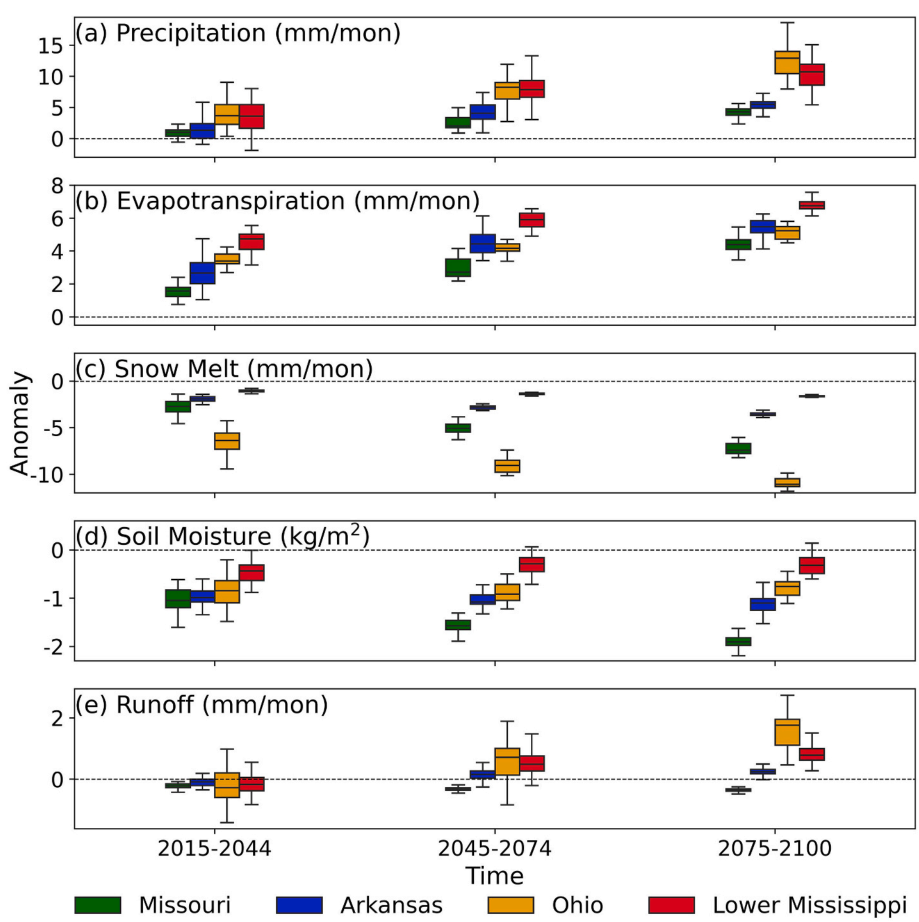


**Fig. 7.** Box plot of the annual mean anomalies under SSP3–7.0 simulations from CESM2 for the basin average (a) precipitation, (b) evapotranspiration, (c) snow melt, (d) soil moisture, and (e) runoff. The anomalies are calculated with respect to the reference period (1971–2000). (For interpretation of the references to colour in this figure legend, the reader is referred to the web version of this article.)

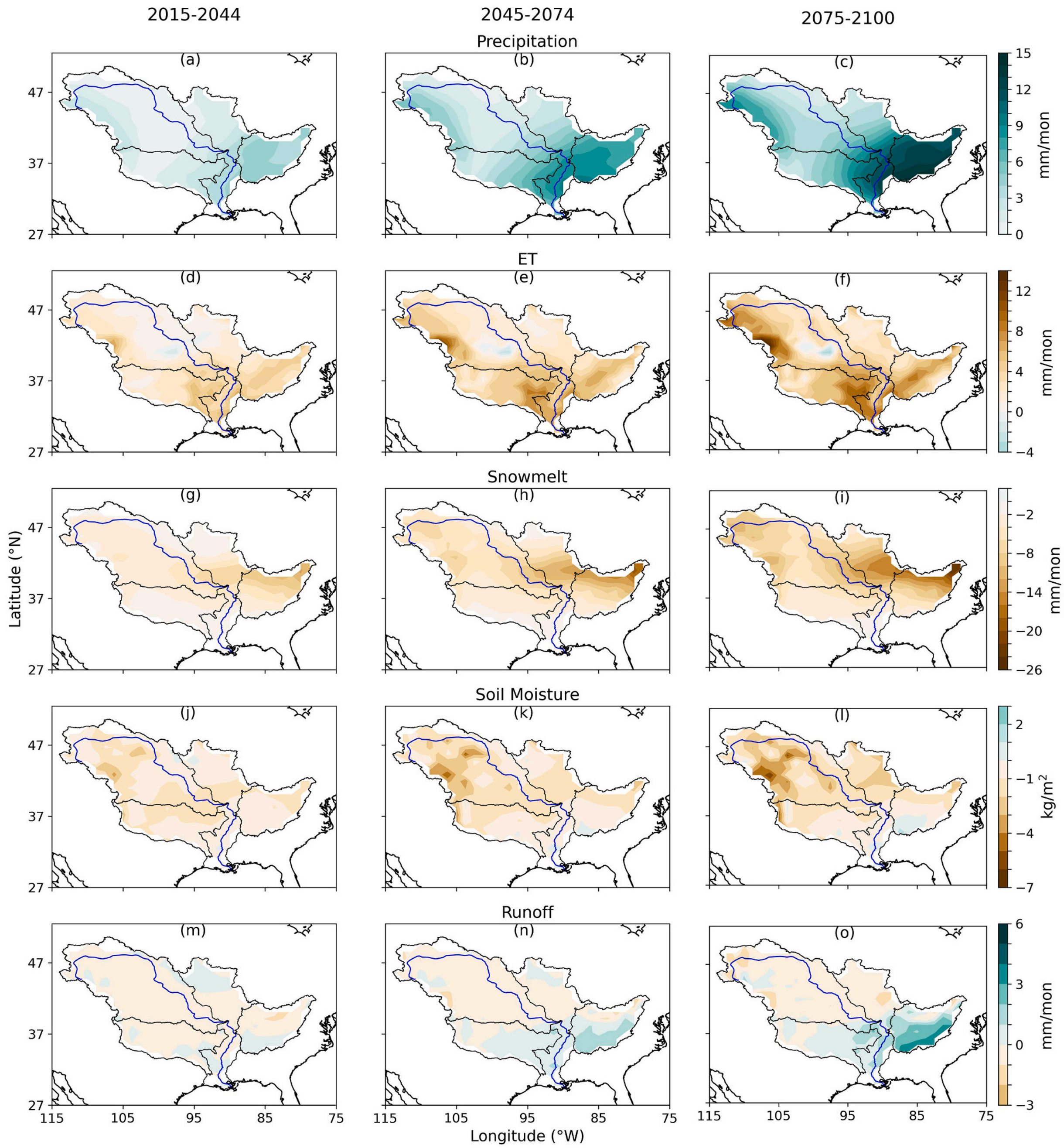


**Fig. 8.** Maps of change in magnitude during the early, mid, and late 21st century with respect to the reference period for the mean (a-c) precipitation, (d-f) evapotranspiration, (g-i) snowmelt, (j-l) soil moisture, and (m-o) runoff over the MRB.

period (Fig. 8d-f). There is a larger decrease in the mean value of snowmelt in the Missouri (up to 8 mm/month), and the Ohio River basin (up to 12 mm/month) in the mid to late 21st century (Fig. 8g-i). The mean value of soil moisture decreases by up to 2, 2, and 1 kg/m$^2$, respectively, in the Missouri, Arkansas, and Ohio River basins but the decreases are less pronounced (<1 kg/m$^2$) in the Lower Mississippi River basin during the 21st century relative to the mean value in the reference period (Fig. 8j-l). Finally, the projected mean runoff shows a large increase by 4 and 2 mm/month, respectively, over the Ohio and Lower Mississippi River basins but the changes are less pronounced (within $\pm$0.7 mm/month) for the Missouri and the Arkansas River basins (Figs. 8m-o).

### 3.5. Seasonality of future basin hydroclimate

To determine the influence of hydroclimate forcing seasonality on future discharge changes in the basin, we first compare the simulated climatological annual cycles for precipitation (Fig. 9a-d), ET (9e-h), snowmelt (9i-l), soil moisture (9 m-p), and runoff (9q-t). Precipitation and ET are projected to increase in the 21st century over all the tributary basins (Fig. 9a-h). In contrast, snowmelt is projected to decrease between November and May in the 21st Century for all the tributary basins (Fig. 9i-l). Soil moisture also decreases during the 21st century in all tributary basins, although the decrease is less prominent for August through December over the Ohio and Lower Mississippi River basins (Fig. 9m-p). The Missouri and Arkansas River basins do not show any appreciable changes in the runoff because of a weaker increase in precipitation minus ET in all the months although a significant reduction of

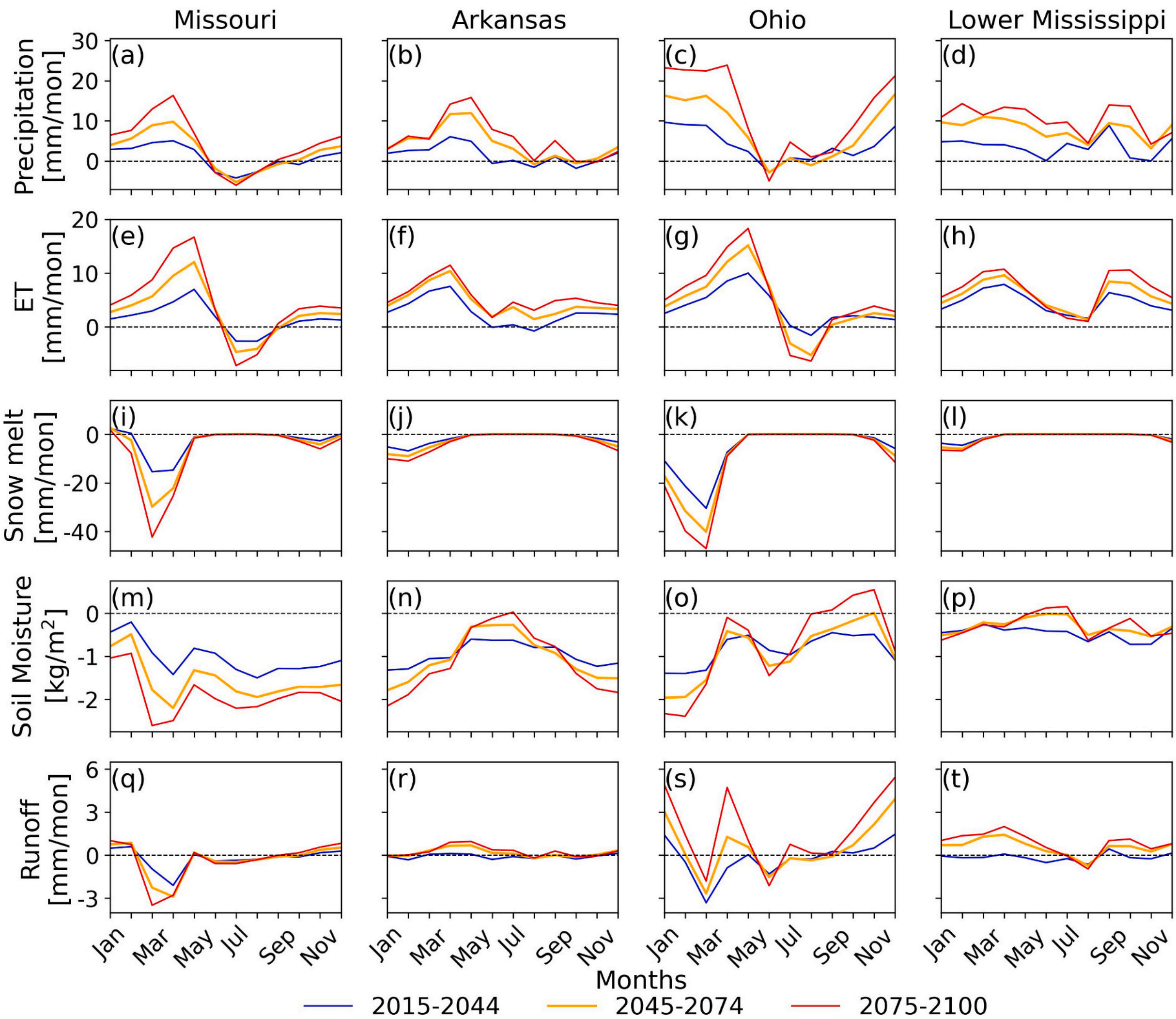


**Fig. 9.** Climatological annual cycles for change of basin average (a-d) precipitation, (e-h) evapotranspiration, (i-l) snowmelt, (m-p) soil moisture, and (q-t) runoff during the early, mid, and late 21st-century relative to the reference period.

snowmelt results in a decrease in runoff during March and April over the Missouri River basin (Fig. 9a, b, e, f, I, q, and r). A large increase in precipitation minus ET over the Ohio River basin results in an increase in runoff during September through May although we note that a significant decrease in snowmelt reduces runoff in February and March (Fig. 9c, g, k, and s). Increased precipitation minus ET in the winter and spring of the 21st century over the Lower Mississippi River basin results in an increase in runoff (Fig. 9d, h, l, and t).

The projected discharge in the 21st century shows a strong seasonal variation across the tributary basins (Fig. 10). The 21st-century discharge in the Missouri and Arkansas River basins do not show any appreciable trend in all the seasons except a decreasing trend in the spring over the Missouri River basin (Fig. 10a, b). The Ohio River basin shows an increasing trend of discharge in the winter, summer, and fall but a decreasing trend for the spring discharge (Fig. 10c). Finally, the Lower Mississippi River discharge is projected to increase throughout the 21st century in all seasons, with the largest increases in the winter (Fig. 10d). To diagnose the drivers of these changes in seasonal discharge, we assess the yearly variation in the seasonal total of precipitation, ET, snowmelt, soil moisture, and runoff over each tributary basin from 1930 through 2100 (Figs. S5 through S9) and summarize the key hydroclimate changes projected for each basin in Table 2.

In the Missouri River basin, precipitation increases in winter and spring, but a significant reduction of snowmelt occurs in spring leading to an increase (decrease) of runoff during the winter (spring) (Figs. S5a, S7a, and S9a). Notably, the projected spring runoff, on average, accounts for a large fraction (39 %) of the yearly total runoff over the basin during 2015–2100 (Fig. S10). During summer and fall, no appreciable trend in runoff is projected for the 21st century (Fig. S9a). Soil moisture shows a decreasing trend for all the seasons (Fig. S8a). Together, a significantly decreasing trend of discharge in the spring with no appreciable trend of discharge in the winter, summer, and fall is projected over the Missouri River basin (Fig. 10a). In the Arkansas River basin, during spring, an increase of precipitation minus ET results in an increasing trend of runoff during the 21st century (Fig. S5b, S6b, and S9b). No trend of runoff is projected for the winter, fall, and summer seasons (Fig. S9b) for the basin. Soil moisture mostly shows a decreasing trend during all seasons (Fig. S8b). Thus, there is no appreciable trend in discharge in all the seasons in the Arkansas River basin (Fig. 10b). In the Ohio River basin, a stronger increase of precipitation minus ET results in an increasing trend of runoff during winter and fall despite a decreasing trend of snowmelt in winter during the 21st century (Fig. S5c, S6c, S7c, and S9c). Importantly, a stronger increase in ET coupled with a decrease in snowmelt during the spring results in a decrease in runoff over the basin (Fig. S6c, S7c, and S9c). We note that spring runoff, on average, accounts for a relatively small fraction (12 %) of the yearly total runoff during 2015–2100 over the Ohio River basin (Fig. S10). Soil moisture shows a decreasing trend in all the seasons during the 21st century

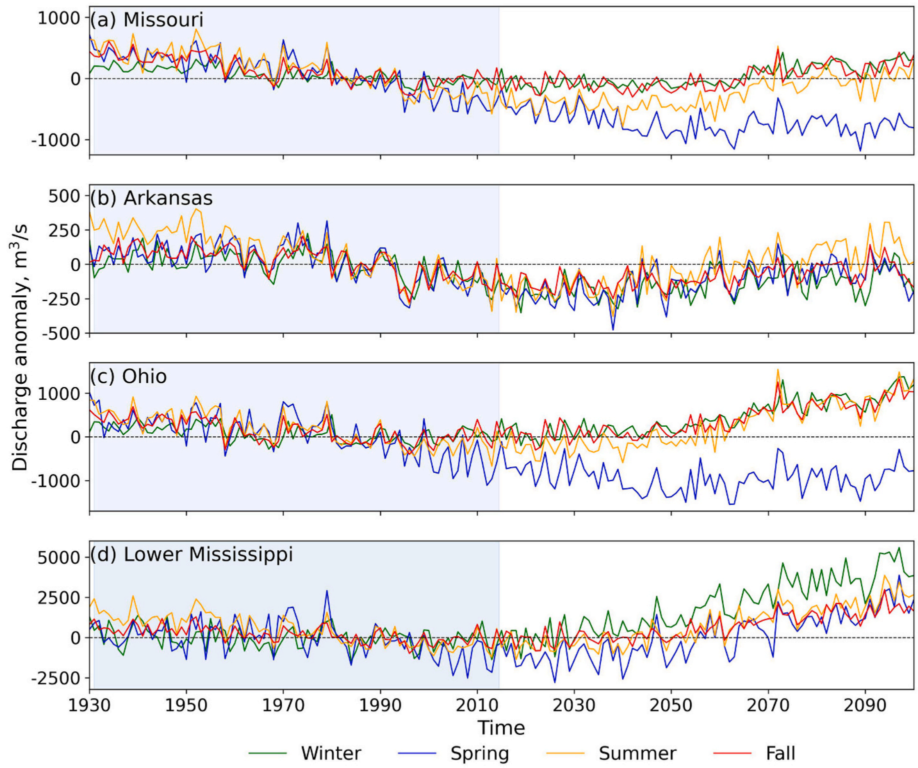


**Fig. 10.** Time series of seasonal mean discharge anomalies under the historical (shaded blue) and SSP3–7.0 simulations from CESM2 at the outlet of each tributary basin during the winter (DJF), spring (MAM), summer (JJA), and fall (SON). (For interpretation of the references to colour in this figure legend, the reader is referred to the web version of this article.)

**Table 2**
Summary of hydroclimate variable changes by season (winter: DJF, spring: MAM, summer: JJA, fall: SON) projected for the 21st century in each tributary basin. Bold blue font indicates an increasing trend; italic bold font in red indicates a decreasing trend; bold font in black indicates no trend.

| BASIN | PRECIPITATION | ET | SNOWMELT | SOIL MOISTURE | RUNOFF |
|---|---|---|---|---|---|
| Missouri | **DJF**, **MAM**, ***JJA***, **SON** | **DJF**, **MAM**, ***JJA***, **SON** | **DJF**, ***MAM***, **JJA**, **SON** | ***DJF***, ***MAM***, ***JJA***, ***SON*** | **DJF**, ***MAM***, **JJA**, **SON** |
| Arkansas | **DJF**, **MAM**, **JJA**, **SON** | **DJF**, **MAM**, **JJA**, **SON** | ***DJF***, **MAM**, **JJA**, **SON** | ***DJF***, ***MAM***, **JJA**, ***SON*** | **DJF**, **MAM**, **JJA**, **SON** |
| Ohio | **DJF**, **MAM**, **JJA**, **SON** | **DJF**, **MAM**, ***JJA***, **SON** | ***DJF***, ***MAM***, **JJA**, **SON** | ***DJF***, ***MAM***, ***JJA***, **SON** | **DJF**, ***MAM***, **JJA**, **SON** |
| Lower Mississippi | **DJF**, **MAM**, **JJA**, **SON** | **DJF**, **MAM**, **JJA**, **SON** | ***DJF***, **MAM**, **JJA**, **SON** | **DJF**, **MAM**, **JJA**, **SON** | **DJF**, **MAM**, **JJA**, **SON** |

(Fig. S8c). Together, discharge in the Ohio River shows an increasing trend during winter, summer, and fall and a decreasing trend during spring (Fig. 10c). For the Lower Mississippi River basin, both precipitation and ET are projected to increase for all the seasons in the 21st century (Fig. S5d, and S6d). Soil moisture does not show any appreciable trend for all the seasons (Fig. S8d). A larger increase in precipitation minus ET results in an increasing trend of runoff and discharge for all the seasons in the 21st century (Fig. S5d, S6d, S9d, and 10d).

Finally, we assess the spatial patterns of hydroclimate change in each season to indicate the contributions of each variable to MRB discharge (Figs. 11–12 and S11-S13). Precipitation in the winter, spring, and fall is projected to increase in the early 21st century compared to the reference period in all the tributary basins, a signal which further intensifies towards the late century (Figs. 11a-f, and 11j-l). In contrast, precipitation in the summer is projected to decrease over Missouri and Ohio River basins but increase in Arkansas and the Lower Mississippi River basins during the 21st century compared to the reference period (Fig. 11g-i). An increase in ET during the winter, spring, and fall is projected over all the basins in the 21st century (Fig. 12a-f, j-l). ET in the summer is projected to decrease in the Missouri and Ohio River basins but increase in Arkansas, and the Lower Mississippi River basins in the 21st century (Fig. 12g-i). Snowmelt shows a decrease in the winter and spring seasons during the early 21st century over the Missouri and Ohio River basins (Fig. 10a-c). The soil moisture shows a decreasing trend in all the seasons over the Missouri and Arkansas River basins in the 21st century (Fig. 11a-l). The Ohio River basin shows a large decrease in soil moisture

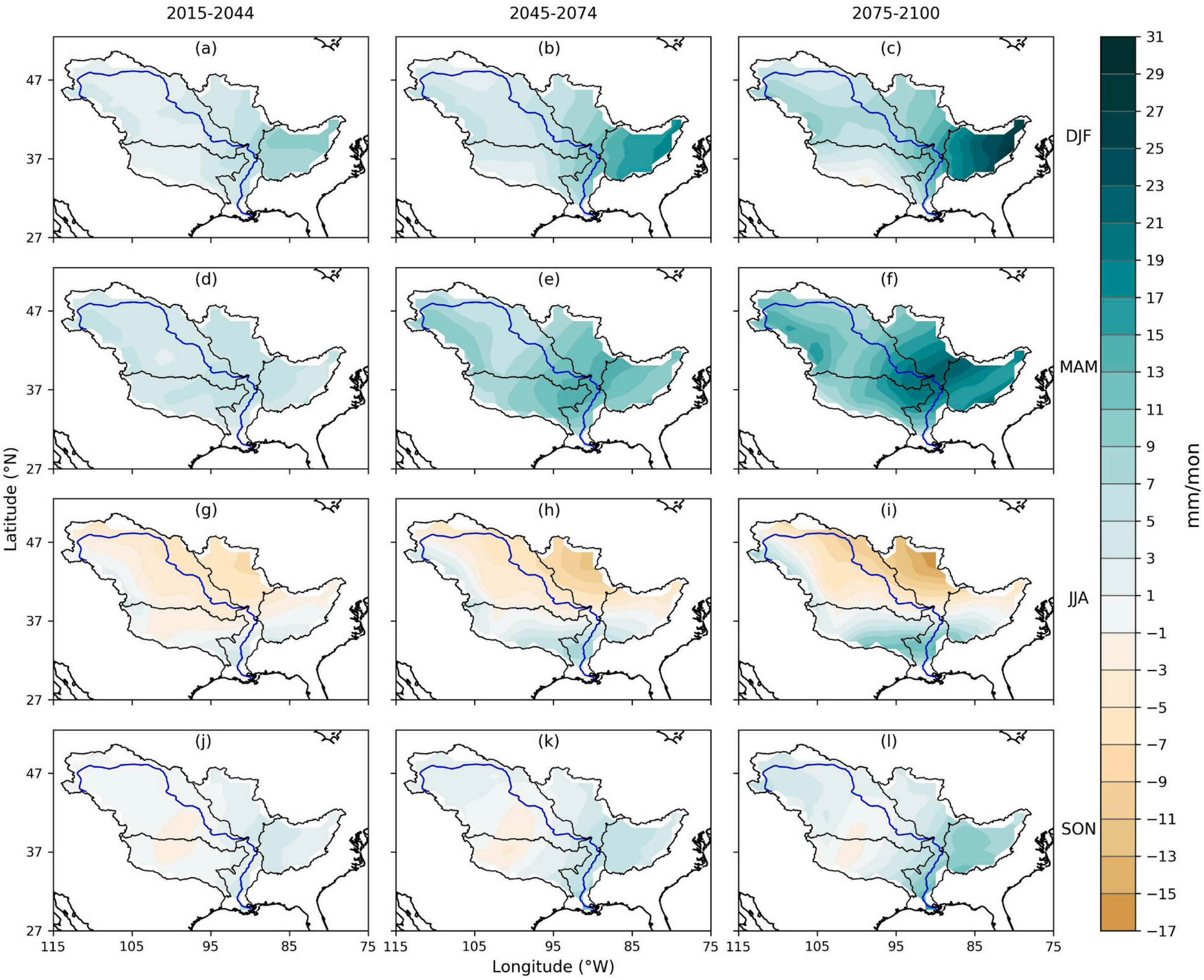


**Fig. 11.** Maps of seasonal change for the early, mid, and late 21st century with respect to the reference period for the ensemble mean precipitation during (a-c): DJF, (d-f): MAM, (g-i): JJA, and (j-l): SON over the MRB.

during the winter and spring with insignificant changes during the summer and fall seasons (Fig. 11a-l). The Lower Mississippi River basin shows a minor change in soil moisture in all seasons (Fig. 11a-l). The projected changes in runoff are less pronounced during all the seasons over the Missouri and Arkansas River basins except for a strong decrease (up to 3 mm/mon averaged over the basin) in the spring season over the Missouri River basin (Fig. 12a-l). Runoff over the Ohio River basin is projected to increase during the fall, winter, and spring (Fig. 12a-f, j-l). The Lower Mississippi River basin shows a moderate increase in runoff in all the seasons during the mid and late 21st century (Fig. 12a-l).

### *3.6. Extreme value analysis for Mississippi river discharge*

The annual peak flow and return period of observed instrumental, historical, and projected discharge for the Mississippi River at Vicksburg are shown in Fig. 13. Compared to the observed discharge, there is a shift towards higher magnitudes in the simulated discharge as a function of the return period (Fig. 13). Discharge in the late 21st century at Vicksburg is projected to increase by 1151 (2 %) and 1942 (3 %) $m^3/s$ compared to that in the historical years at a return period of 100 and 1000 years, respectively (Table S3). Notably, neither the observed nor the simulated discharge exceed the Project Design Flood Level (DFL) up to 1000-year flooding.

## 4. Discussion & conclusions

This study utilizes simulations from the CESM2 Large Ensemble to assess the climate change impacts on river discharge in the 21st century. We explore future changes in key hydroclimate variables such as precipitation, ET, snow melt, soil moisture, and runoff across all the major tributary basins in the MRB under the influence of SSP3–7.0, a high emissions scenario, as well as how these changes alter future discharge variability in the basin. We also analyze how climate change impacts hydroclimate seasonality, which is likely to affect discharge variability in the MRB during the 21st century.

A validation of CESM2's discharge compared to USGS observations suggests, the mean of the simulated discharge is 11 % higher compared to the mean observed discharge for the lower Mississippi River at Vicksburg; the mean simulated discharge in different seasons shows wetter conditions compared to observation represented by reasonable biases (4–7 %) during winter, spring, and summer but a large bias (44 %) during fall (Fig. 2). The simulations show up to a 10 % decrease over the Missouri and Arkansas Rivers and up to 10 % increase over the Ohio and Mississippi Rivers in the mean of the ensemble mean monthly discharge during the early, mid, and late 21st century relative to the reference mean (Fig. 3). The climatological annual cycle shows a wide range of variability in monthly discharge during the 21st century relative to the reference period at the selected gauges. The early, mid, and late 21st century monthly discharge shows a maximum decrease by 17, 23, and 21 % and a maximum increase by 5, 11, and 21 % across the tributary

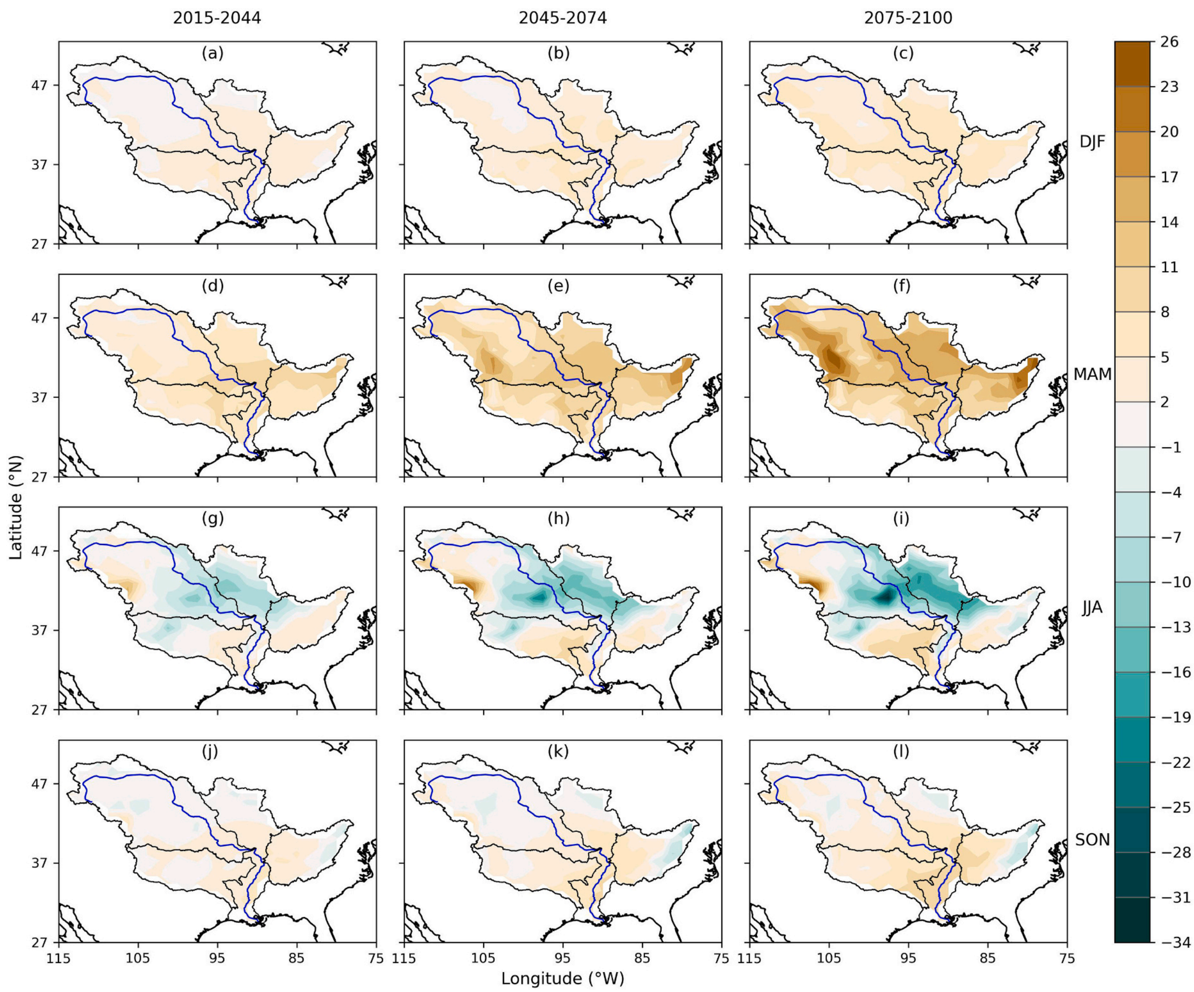


**Fig. 12.** Maps of seasonal change for the early, mid, and late 21st century with respect to the reference period for the ensemble mean ET during (a-c): DJF, (d-f): MAM, (g-i): JJA, and (j-l): SON over the MRB.

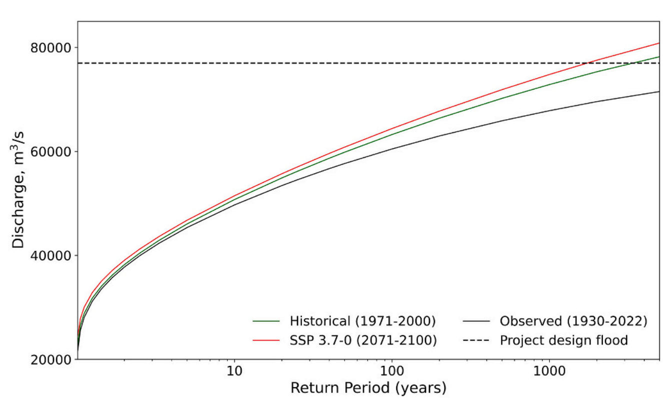


**Fig. 13.** Annual peak flow versus return period of the observed instrumental discharge (black), historical discharge (green), and projected discharge (red) for the Mississippi River at Vicksburg. The simulated discharge is bias-corrected and includes a blend of 40 members for the historical and future periods. (For interpretation of the references to colour in this figure legend, the reader is referred to the web version of this article.)

basins relative to the reference period (Fig. 4). On a yearly scale, the Missouri and Arkansas Rivers show a decreasing trend during the early 21st century and an increasing trend during the mid and late 21st century, although the discharge magnitudes are mostly less than the reference period average (Fig. 5). In contrast, the annual discharge at the Ohio and Mississippi Rivers does not show any appreciable trend during the early 21st century, but increases throughout the mid and late 21st century with the largest increases for the two rivers being 12 % and 17 %, respectively (Fig. 5).

Different hydroclimate variables are projected to modulate the 21st century discharge in the MRB. ET is projected to increase throughout the 21st century over all the tributary river basins, but the precipitation outpaces ET in the mid and late 21st century over the Ohio and Lower Mississippi River basins (Figs. 6a-b; 7a-b; and 8a-f). As expected under warming atmospheric conditions, snowmelt decreases sharply over the Ohio, and Missouri River basins throughout the 21st century showing a maximum reduction of up to 12 and 7 mm/month, respectively (Figs. 6 c,e; 7 c,e; 8 g-i; 8 m-o; and 9 i-l). Finally, soil moisture is also projected to decrease over the Missouri, Arkansas, and Ohio River basins with no significant trend projected for the Lower Mississippi River basin in the 21st century (Figs. 6d; 7d; and 8j-l). Together, these hydroclimate changes converge to result in an increasing runoff trend in the Ohio and the Lower Mississippi River basins and no significant trend of runoff in the Missouri and Arkansas River basins (Figs. 6e; 7e; and 8 m-o).

Strong seasonal changes in hydrological cycle variables are also projected for the tributary river basins during the 21st century (Fig. 9 a-t). A minor increase of precipitation minus ET in all the seasons together with a decrease in spring snowmelt over the Missouri River basin results in a decreased spring discharge whereas the discharge in the other seasons does not show any appreciable trend (Fig. 9a, e; 10a; S5a; S6a; S7a; 11; and 12). The 21st century discharge in the Arkansas River does not show any appreciable trend in all the seasons dictated by a minor increase of precipitation minus ET over the basin (Fig. 9b, f; 10b; S5b; S6b; 11; and 12). Large increase in P-ET occurs over the Ohio River basin in all the seasons during the 21st century (Fig. 9c, g; S5c; S6c; 11; and 12). A large reduction of snowmelt occurs between the late winter and the early spring that reduces runoff in early spring over the basin (Fig. 9k, s; S7c). Together, discharge in the basin shows an increase during the winter, summer, and fall but a decrease during the spring (Fig. 10c). Finally, a large increase in the projected precipitation minus ET results in an increase in runoff and river discharge at all the seasons during the mid and late 21st century in the Lower Mississippi River basin (Figs. 10d; S5d; S6d; S9d; 11; and 12). FFA shows an increase of 1151 $m^3/s$ (or 2 %) in the late 21st-century projected discharge compared to the simulated discharge in the reference period at Vicksburg with a 100-year return period but the project design flood level is not exceeded up to a return period of 1000 years (Fig. 13). This finding is in contrast to Dunne et al., 2022 because they used the RTM (Branstetter, 2003) module for river routing whereas this study uses MOSART (H. Li et al., 2013; H.-Y. Li et al., 2015).

We posed the following questions in our introduction, which we briefly review here: *1) How well does the CESM2 LENS simulate observed Mississippi River discharge (means, extremes, and seasonality) in the historical period?* CESM2 simulates mean and high flows with high accuracy, but exhibits large biases in simulated low flows. The bias of the simulated discharge is low (4–7 %) in all the seasons except the fall when there is a large bias of 44 %. *2) How do Mississippi River discharge statistics change under SSP3–7.0 during the 21st century?* Future projections show a decrease (as much as −10 %) in mean discharge during the early, mid, and late 21st century relative to the reference mean for the Missouri and Arkansas. Mean discharge for the Ohio and Lower Mississippi basins shows a maximum increase of 4 %, and 10 % during the mid and late 21st century relative to the reference mean. *3) How do the various components of the hydrological cycle contribute to changes in discharge in each tributary basin under the high emissions scenario?* Higher increase in precipitation compared to ET over the Lower Mississippi River basin drives an overall increase in average discharge. There is a large decrease in snowmelt over the Ohio River basin which is overshadowed by the increase in precipitation relative to ET, resulting in a net increase in average discharge. *4) How does the seasonality of hydroclimate drivers affect discharge changes over the tributary basins?* A decreasing trend in spring snowmelt over the Ohio and Missouri River basins results in a large reduction of spring discharge. And, finally, *5) Does the future flooding exceed the design discharge of the MR&T project?* Extreme value analysis shows an increase in the projected discharge at Vicksburg compared to the historical years but the Project Design Flood Level is not exceeded at a 100-year return period.

Our study provides information on projected trends in Mississippi River discharge using a state-of-the-art model ensemble, diagnoses hydroclimate drivers of those trends, and calculates percentage changes in flows in the basin. These findings represent an important advance in our understanding of how and why the streamflow of the largest river in North America responds under a high emissions scenario. Despite biases in CESM2's simulated discharge values, we believe our analyses of future trends remain crucial for managers and government authorities to plan and implement appropriate flood and low-flow mitigation.

Our study harbors important limitations and uncertainties. We use only the CESM2 LENS2 projections for future hydroclimate in the MRB. Although we utilize a large 50-member ensemble, using a single emissions scenario from a single model does not ensure a full investigation of outcomes given different plausible human behaviors and different emission levels (Baumberger et al., 2017; Cheung et al., 2016). A multimodel ensemble analysis is required to reduce the uncertainty in the simulated output and increase the robustness (Sisco et al., 2022; Baumberger et al., 2017; Cheung et al., 2016) of model projections; such work is ongoing amongst the authors of this manuscript. Secondly, MOSART – the river transport and routing model in CESM2 – does not consider the influence of human interventions on the river (as discussed in Dunne et al., 2022). To generate more robust projections of flood risk, a higher resolution hydro-morphological study for the MRB considering different interventions on the river will be required. Such extension research to pinpoint the hydrodynamic changes with proper attention to seasonal variation of the drivers of both flooding and low flows is sorely needed, an area we hope to address in forthcoming work.

Taken together, these findings provide a new, large model ensemble perspective on future hydroclimate change in the MRB, and partition the relative roles of specific hydrological cycle components in the basin under anthropogenic warming. In CESM2, the increase of precipitation outpaces that of ET, leading to an increasing trend in runoff in the 21st century over the Ohio and Lower Mississippi River basins. Seasonal analysis reveals a sizable reduction of spring snowmelt, leading to a decrease in runoff and discharge over the Missouri and Ohio Rivers basins, but, interestingly, the impacts of decreased snowmelt are overshadowed by the overall increase in rainfall. Future work must monitor these hydrological forcings in the basin via both remote sensing and ground-based observations to assess the accuracy (and thus reliability) of CESM2's projections and seasonality. We conclude and assert that CESM2 projections for the 21st century unequivocally show an increasing trend of average discharge in the Lower Mississippi River, corroborating other recent modeling studies, and underscoring the urgency of updates to flood hazard management in the basin (Tao et al., 2014; Lewis et al., 2022; Dunne et al., 2022). If hydroclimate shifts over the MRB towards overall wetter conditions alongside strong changes in seasonality, implications for water resources management include increased flood vulnerability and disruption of shipping, agriculture, fisheries, and industry in the MRB (Eugene Turner, 2022). CESM2 projections further support the need for re-evaluation of the MR&T project design flood and shifts in return periods with warming in the 21st century. Structural modifications including retrofitting (Dunne et al., 2022) as well as non-structural solutions, including citizen awareness-building surrounding future flooding risks in their region, and careful monitoring of flood control structure operations season to season will all improve the resilience of this critical U.S. resource over the coming decades (USACE, 2023). However, to make progress on these fronts, forthcoming work must bridge divides between the GCM and computational hydrology communities to link large-scale climate change to local inundation models. It is our hope that this work takes an important first step towards establishing those linkages, and provides a starting baseline for interrogating the links between hydroclimate changes and river discharge in the MRB throughout the 21st century.

## CRediT authorship contribution statement

**M.R. Haider:** Writing – review & editing, Writing – original draft, Visualization, Validation, Software, Methodology, Investigation, Formal analysis, Data curation, Conceptualization. **S.G. Dee:** Writing – review & editing, Writing – original draft, Supervision, Project administration, Methodology, Investigation, Funding acquisition, Conceptualization. **J. Doss-Gollin:** Writing – original draft, Supervision, Investigation, Funding acquisition, Conceptualization. **K.B.J. Dunne:** Methodology, Investigation. **S.E. Muñoz:** Writing – original draft, Supervision, Methodology, Investigation, Formal analysis, Conceptualization.

## Declaration of competing interest

The authors declare that they have no competing financial interests or personal relationships that could influence the work.

## Acknowledgements

The research was supported by the US National Science Foundation grant number CLD-2147781 (Haider, Dee, Doss-Gollin, and Muñoz).

## Appendix A. Supplementary data

Supplementary data to this article can be found online at https://doi.org/10.1016/j.gloplacha.2025.104742.

## Data availability

Climate model data from CESM2 was downloaded from the Globally Accessible Data Environment (GLADE, https://arc.ucar.edu/knowledge_base/68878466) repository of the National Center for Atmospheric Research. The scripts supporting the findings of this study are available via: https://github.com/rezaulg/CESM2-projection-Mississippi-discharge.git.

## References

Aguayo, Rodrigo, León-Muñoz, Jorge, Garreaud, René, Montecinos, Aldo, 2021. Hydrological droughts in the Southern Andes (40-45°S) from an ensemble experiment using CMIP5 and CMIP6 models. Sci. Rep. 11 (1), 5530.
Alexander, Jason Scott, Wilson, Richard C., Reed Green, W., 2012. A Brief History and Summary of the Effects of River Engineering and Dams on the Mississippi River System and Delta, vol. 1375. US Department of the Interior, US Geological Survey.
Barnett, A., Fargione, J., Smith, M.P., 2016. Mapping trade-offs in ecosystem services from reforestation in the Mississippi Alluvial Valley. BioScience 66 (3), 223–237. https://doi.org/10.1093/biosci/biv181.
Baumberger, Christoph, Knutti, Reto, Hadorn, Gertrude Hirsch, 2017. Building confidence in climate model projections: an analysis of inferences from fit. Wiley Interdiscip. Rev. Clim. Chang. 8 (3), e454.
Bian, Guodong, Zhang, Jianyun, Song, Mingming, Qian, Xin, Guan, Tiesheng, Wang, Guoqing, 2023. Projections of flood regime changes over the upper-middle Huaihe River Basin in China based on CMIP6 models. Front. Environ. Sci. Eng. China 11 (August), 1247753.
Branstetter, Marcia L., 2003. Continental runoff dynamics in the community climate system model 2 (CCSM2) control simulation. J. Geophys. Res. 108 (D17). https://doi.org/10.1029/2002jd003212.
Cheung, William W.L., Frölicher, Thomas L., Asch, Rebecca G., Jones, Miranda C., Pinsky, Malin L., Reygondeau, Gabriel, Rodgers, Keith B., et al., 2016. Building confidence in projections of the responses of living marine resources to climate change. ICES J. Marine Sci. J. Du Conseil 73 (5), 1283–1296.
Coelho, G.A., Ferreira, C.M., Johnston, J., Kinter III, J.L., Dollan, I.J., Maggioni, V., 2022. Potential impacts of future extreme precipitation changes on flood engineering design across the contiguous United States. Water Resour. Res. 58, e2021WR031432. https://doi.org/10.1029/2021WR031432.
Danabasoglu, G., Lamarque, J.-F., Bacmeister, J., Bailey, D.A., DuVivier, A.K., Edwards, J., Emmons, L.K., et al., 2020. The community earth system model version 2 (CESM2). J. Adv. Model. Earth Syst. 12 (2). https://doi.org/10.1029/2019ms001916.
DeHaan, Henry, Stamper, Jeffery, Walters, Bret, 2012. Mississippi River and Tributaries System 2011 Post-Flood Report: Documenting the 2011 Flood, the Corps' Response, and the Performance of the MR&T System.
Deser, Clara, Knutti, Reto, Solomon, Susan, Phillips, Adam S., 2012. Communication of the role of natural variability in future North American climate. Nat. Clim. Chang. 2 (11), 775–779.
Deser, C., Lehner, F., Rodgers, K.B., Ault, T., Delworth, T.L., DiNezio, P.N., Fiore, A., et al., 2020. Insights from Earth system model initial-condition large ensembles and future prospects. Nat. Clim. Chang. 10 (4), 277–286.
Dunne, K.B.J., Dee, S.G., Reinders, J., Muñoz, S.E., Nittrouer, J.A., 2022. Examining the impact of emissions scenario on lower Mississippi River flood hazard projections. Environ. Res. Commun. https://doi.org/10.1088/2515-7620/ac8d53.
Eugene Turner, R., 2022. Variability in the discharge of the Mississippi River and Tributaries from 1817 to 2020. PLoS One 17 (12), e0276513.
Foley, Jonathan A., Kucharik, Christopher J., Twine, Tracy E., Coe, Michael T., Donner, Simon D., 2004. Land use, land cover, and climate change across the Mississippi Basin: impacts on selected land and water resources. In: Ecosystems and Land Use Change. Geophysical Monograph. American Geophysical Union, Washington, D. C, pp. 249–261.
Frans, Chris, Istanbulluoglu, Erkan, Mishra, Vimal, Munoz-Arriola, Francisco, Lettenmaier, Dennis P., 2013. Are climatic or land cover changes the dominant cause of runoff trends in the Upper Mississippi River Basin? Geophys. Res. Lett. https://doi.org/10.1002/grl.50262.
Georgakakos, A., Fleming, P., Dettinger, M., Peters-Lidard, C., Richmond, Terese, Reckhow, K., White, K., Yates, D., 2014. Ch. 3: "Water Resources". In: Melillo, J.M., Richmond, Terese, Yohe, G.W. (Eds.), Climate Change Impacts in the United States: The Third National Climate Assessment. U.S. Global Change Research Program, pp. 69–112. https://doi.org/10.7930/J0G44N6T.
Gilleland, E., Katz, R.W., 2016. extRemes 2.0: An Extreme Value Analysis Package in R. Journal of Statistical Software 72 (8), 1–39. https://doi.org/10.18637/jss.v072.i08.
Hanittinan, Patinya, Tachikawa, Yasuto, Ram-Indra, Teerawat, 2020. Projection of hydroclimate extreme indices over the Indochina Region under climate change using a large single-model ensemble. Int. J. Climatol. 40 (6), 2924–2952.
Hawkins, Ed, Sutton, Rowan, 2009. The potential to narrow uncertainty in regional climate predictions. Bull. Am. Meteorol. Soc. 90 (8), 1095–1108.
Huang, Shaochun, Kumar, Rohini, Rakovec, Oldrich, Aich, Valentin, Wang, Xiaoyan, Samaniego, Luis, Liersch, Stefan, Krysanova, Valentina, 2018. Multimodel assessment of flood characteristics in four large River Basins at global warming of 1.5, 2.0 and 3.0 K above the pre-industrial Level. Environ. Res. Lett. 13 (12), 124005.
Ivanov, Martin Aleksandrov, Luterbacher, Jürg, Kotlarski, Sven, 2018. Climate model biases and modification of the climate change signal by intensity-dependent bias correction. J. Clim. 31 (16), 6591–6610.
Jha, Manoj, 2004. Impacts of climate change on streamflow in the Upper Mississippi River Basin: a regional climate model perspective. J. Geophys. Res. https://doi.org/10.1029/2003jd003686.
Kay, J.E., Deser, C., Phillips, A., Mai, A., Hannay, C., Strand, G., Arblaster, J.M., et al., 2015. The community earth system model (CESM) large ensemble project: a community resource for studying climate change in the presence of internal climate variability. Bull. Am. Meteorol. Soc. 96 (8), 1333–1349.
Kolpin, D., 2000. Importance of the Mississippi River Basin for investigating agricultural–chemical contamination of the hydrologic cycle. Sci. Total Environ. 248 (2–3), 71–72.
Konstali, K., Spengler, T., Spensberger, C., Sorteberg, A., 2024. Linking future precipitation changes to weather features in CESM2-LE. J. Geophys. Res. Atmos. 129, e2024JD041190. https://doi.org/10.1029/2024JD041190.
Kumar, Sanjiv, Dewes, Candida F., Newman, Matthew, Duan, Yanan, 2023. Robust changes in North America's hydroclimate variability and predictability. Earth's Future 11 (4), e2022EF003239.
Lewis, James W., 2019. Mississippi River and Tributaries Future Flood Conditions.
Lewis, James W., Lytle, Sara E., Tavakoly, Ahmad A., 2022. Climate change projections of continental-scale streamflow across the Mississippi River Basin. Theor. Appl. Climatol. 151 (3), 1013–1034.
Li, Hongyi, Wigmosta, Mark S., Huan, Wu, Huang, Maoyi, Ke, Yinghai, Coleman, André M., Ruby Leung, L., 2013. A physically based runoff routing model for land surface and Earth system models. J. Hydrometeorol. 14 (3), 808–828.
Li, Hong-Yi, Ruby Leung, L., Getirana, Augusto, Huang, Maoyi, Huan, Wu, Yubin, Xu, Guo, Jiali, Voisin, Nathalie, 2015. Evaluating global streamflow simulations by a physically based routing model coupled with the community land model. J. Hydrometeorol. 16 (2), 948–971.
Ma, W., Norris, J., Chen, G., 2020. Projected changes to extreme precipitation along north American west coast from the CESM large ensemble. Geophys. Res. Lett. 47, e2019GL086038. https://doi.org/10.1029/2019GL086038.
Mankin, Justin S., Viviroli, Daniel, Singh, Deepti, Hoekstra, Arjen Y., Diffenbaugh, Noah S., 2015. The potential for snow to supply human water demand in the present and future. Environ. Res. Lett. ERL 10 (11), 114016.
Mankin, Justin S., Lehner, Flavio, Coats, Sloan, McKinnon, Karen A., 2020. The value of initial condition large ensembles to robust adaptation decision-making. Earth's Future 8 (10), e2012EF001610.
Martel, J.-L., Brissette, F., Troin, M., Arsenault, R., Chen, J., Su, T., Lucas-Picher, P., 2022. CMIP5 and CMIP6 model projection comparison for hydrological impacts over North America. Geophys. Res. Lett. 49 (15), e2022GL098364.
Meade, Robert H., Moody, John A., 2009. Causes for the decline of suspended-sediment discharge in the Mississippi River System, 1940-2007. Hydrol. Process. https://doi.org/10.1002/hyp.7477.
Mishra, Vimal, Cherkauer, Keith A., Niyogi, Dev, Lei, Ming, Pijanowski, Bryan C., Ray, Deepak K., Bowling, Laura C., Yang, Guoxiang, 2010. A regional scale assessment of land use/land cover and climatic changes on water and energy cycle in the Upper Midwest United States. Int. J. Climatol. 30 (13), 2025–2044.
Mudryk, L.R., Kushner, P.J., Derksen, C., 2014. Interpreting observed Northern hemisphere snow trends with large ensembles of climate simulations. Clim. Dyn. 43 (1–2), 345–359.
Munoz, Samuel E., Dee, Sylvia G., 2017. El Niño increases the risk of lower Mississippi River flooding. Sci. Rep. 7 (1), 1772.
Munoz, S., Giosan, L., Therrell, M., et al., 2018. Climatic control of Mississippi River flood hazard amplified by river engineering. Nature 556, 95–98. https://doi.org/10.1038/nature26145.
Muñoz, Samuel E., Dee, Sylvia G., Xinyue Luo, M., Haider, Rezaul, O'Donnell, Michelle, Parazin, B., Remo, Jonathan W.F., 2023. Mississippi River low-flows: context, causes, and future projections. Environ. Res. Clim. 2 (3), 031001.
O'Donnell, M., Murphy, K., Doss-Gollin, J., Dee, S., Munoz, S., 2024. Evaluation of hydroclimatic biases in the Community Earth System Model (CESM1) within the Mississippi River basin. Hydrol. Earth Syst. Sci. Discuss. https://doi.org/10.5194/hess-2024-153 [preprint]. in review.
NOAA PSL.. CPC Unified Gauge-Based Analysis of Daily Precipitation over CONUS data [Dataset]. PSL Climate Data Repository. https://psl.noaa.gov/repository/entry/show?entryid=2829f7f8-6473-48ec-bdd9-698e20eadfcf.
Otto-Bliesner, Bette L., Brady, Esther C., Fasullo, John, Jahn, Alexandra, Landrum, Laura, Stevenson, Samantha, Rosenbloom, Nan, Mai, Andrew, Strand, Gary, 2016. Climate variability and change since 850 CE: an ensemble approach with the community Earth system model. Bull. Am. Meteorol. Soc. 97 (5), 735–754.
Peterson, Thomas C., Heim, Richard R., Hirsch, Robert, Kaiser, Dale P., Brooks, Harold, Diffenbaugh, Noah S., Dole, Randall M., et al., 2013. Monitoring and understanding changes in heat waves, cold waves, floods, and droughts in the United States: state of knowledge. Bull. Am. Meteorol. Soc. 94 (6), 821–834.
Pinter, Nicholas, Heine, Reuben A., 2005. Hydrodynamic and morphodynamic response to river engineering documented by fixed-discharge analysis, Lower Missouri River, USA. J. Hydrol. 302 (1–4), 70–91.

Pinter, Nicholas, Jemberie, Abebe A., Remo, Jonathan W.F., Heine, Reuben A., Ickes, Brian S., 2008. Flood trends and river engineering on the Mississippi River System. Geophys. Res. Lett. https://doi.org/10.1029/2008gl035987.

Pinter, Nicholas, Jemberie, Abebe A., Remo, Jonathan W.F., Heine, Reuben A., Ickes, Brian S., 2010. Cumulative impacts of River Engineering, Mississippi and Lower Missouri Rivers. River Res. Appl. 26 (5), 546–571.

Pitlick, John, 1997. A Regional Perspective of the Hydrology of the 1993 Mississippi River Basin Floods.

Prudhomme, Christel, Giuntoli, Ignazio, Robinson, Emma L., Clark, Douglas B., Arnell, Nigel W., Dankers, Rutger, Fekete, Balázs M., et al., 2014. Hydrological droughts in the 21st Century, hotspots and uncertainties from a global multimodel ensemble experiment. Proc. Natl. Acad. Sci. USA 111 (9), 3262–3267.

Qian, Taotao, Dai, Aiguo, Trenberth, Kevin E., 2007. Hydroclimatic trends in the Mississippi River Basin from 1948 to 2004. J. Clim. 20 (18), 4599–4614.

Rajib, Adnan, Zheng, Qianjin, Golden, Heather E., Qiusheng, Wu, Lane, Charles R., Christensen, Jay R., Morrison, Ryan R., Annis, Antonio, Nardi, Fernando, 2021. The changing face of floodplains in the Mississippi River Basin detected by a 60-year land use change dataset. Sci. Data 8 (1), 1–11.

Rodgers, Keith B., Lee, Sun-Seon, Rosenbloom, Nan, Timmermann, Axel, Danabasoglu, Gokhan, Deser, Clara, Edwards, Jim, et al., 2021. Ubiquity of human-Induced changes in climate variability. Earth Syst. Dynam. 12 (4), 1393–1411.

Rossi, A., Massei, N., Laignel, B., Sebag, D., Copard, Y., 2009. The response of the Mississippi River to climate fluctuations and reservoir construction as indicated by wavelet analysis of streamflow and suspended-sediment load, 1950–1975. J. Hydrol. 377 (3–4), 237–244.

Schilling, Keith E., Jha, Manoj K., Zhang, You-Kuan, Gassman, Philip W., Wolter, Calvin F., 2008. Impact of land use and land cover change on the water balance of a large agricultural watershed: historical effects and future directions. Water Resour. Res. 44 (7). https://doi.org/10.1029/2007wr006644.

Schilling, Keith E., Chan, Kung-Sik, Liu, Hai, Zhang, You-Kuan, 2010. Quantifying the effect of land use land cover change on increasing discharge in the Upper Mississippi River. J. Hydrol. 387 (3–4), 343–345.

Sisco, A.W., Tavakoly, Ahmad A., Kao, Shih-Chich, 2022. Continental-scale changes in discharge of the Mississippi River Basin in response to future hydroclimate projections. In: AGU Fall Meeting, 2022. https://ui.adsabs.harvard.edu/abs/2022AGUFM.H42E1302S/abstract.

Slater, Louise J., Singer, Michael Bliss, Kirchner, James W., 2015. Hydrologic versus geomorphic drivers of trends in flood hazard. Geophys. Res. Lett. 42 (2), 370–376.

Tao, Bo, Tian, Hanqin, Ren, Wei, Yang, Jia, Yang, Qichun, He, Ruoying, Cai, Weijun, Lohrenz, Steven, 2014. Increasing Mississippi River discharge throughout the 21st century influenced by changes in climate, land use, and atmospheric CO2. Geophys. Res. Lett. 41 (14), 4978–4986.

Trenberth, Kevin E., 1999. Conceptual framework for changes of extremes of the hydrological cycle with climate change. Clim. Chang. 42 (1), 327–339.

U.S. Army Corps of Engineers (USACE), 2023. Flood Risk Management. https://www.usace.army.mil/Missions/Civil-Works/Flood-Risk-Management/ (Accessed June 12, 2023).

U.S. Geological Survey (USGS), 2022. North America Watersheds. https://www.sciencebase.gov/catalog/item/4fb697b2e4b03ad19d64b47f (Accessed 2022).

USGS, 2023. USGS Water Data for the Nation. https://nwis.waterdata.usgs.gov/nwis (Accessed April 28, 2023).

van der Wiel, Karin, Kapnick, Sarah B., Vecchi, Gabriel A., Smith, James A., Milly, P.C.D., Jia, Liwei, 2018. 100-year lower Mississippi floods in a global climate model: characteristics and future changes. J. Hydrometeorol. 19 (10), 1547–1563.

Vieira, Michael, J.F., Stadnyk, Tricia, A., 2023. Leveraging global climate models to assess multi-year hydrologic drought. Npj Clim. Atmos. Sci. 6 (1), 1–12. https://doi.org/10.1038/s41612-023-00496-y.

Villarini, Gabriele, Zhang, Wei, 2020. Projected changes in flooding: a continental U.S. perspective. Ann. N. Y. Acad. Sci. 1472 (1), 95–103.

Wiman, Charlotte, Hamilton, Brynnydd, Dee, Sylvia G., Muñoz, Samuel E., 2021. Reduced lower Mississippi River discharge during the medieval era. Geophys. Res. Lett. 48 (3), e2020GL091182.

Yin, S., Gao, G., Li, Y., Xu, Y.J., Turner, R.E., Ran, L., Wang, X., Fu, B., 2023. Long-term trends of streamflow, sediment load and nutrient fluxes from the Mississippi River Basin: impacts of climate change and human activities. J. Hydrol. 616, 128822.

Zheng, Y., Li, S., He, S., Gu, X., 2022. Hydroclimatic intensity change in China during the past decades and its future trend based on CMIP5/6. J. Hydrol. 613 art. no. 128437.